Your Author PDF for *Clinical Science*

We are pleased to provide a copy of the Version of Record of your article. This PDF is provided for your own use and is subject to the following terms and conditions:

- You may not post this PDF on any website, including your personal website or your institution's website or in an institutional or subject-based repository (e.g. PubMed Central).
- You may make print copies for your own personal use.
- You may distribute copies of this PDF to your colleagues provided you make it clear that these are for their personal use only.

Permission requests for re-use or distribution outside of the terms above, or for commercial use, should be sent to editorial@portlandpress.com.

Clinical Science (2014) **127**, 665–677 (Printed in Great Britain) doi: 10.1042/CS20140180

online data

Original Paper

NOD1 receptor is up-regulated in diabetic human and murine myocardium

Patricia PRIETO*, María Teresa VALLEJO-CREMADES†[1], Gemma BENITO†[1], Pilar GONZÁLEZ-PERAMATO‡, Daniel FRANCÉS*, Noelia AGRA*, Verónica TERRÓN*, Silvia GÓNZALEZ-RAMOS*, Carmen DELGADO§, Mariano RUIZ-GAYO¶, Ivette PACHECO**, Juan P. VELASCO-MARTÍN††, Javier REGADERA††, Paloma MARTÍN-SANZ*, Eduardo LÓPEZ-COLLAZO†, Lisardo BOSCÁ* and María FERNÁNDEZ-VELASCO†

*Instituto de Investigaciones Biomédicas Alberto Sols, Centro Mixto CSIC-UAM, Madrid, Spain
†Instituto de Investigación Hospital Universitario La Paz (IDIPAZ), Madrid, Spain
‡Departamento de Anatomía Patológica, Hospital Universitario La Paz, Universidad Autonoma de Madrid, Madrid, Spain
§Centro de Investigaciones Biológicas. Facultad de Medicina, Universidad Complutense de Madrid, Madrid, Spain
¶Universidad CEU San Pablo, Madrid, Spain
**Hospital Militar de Managua, Managua, Nicaragua
††Departamento de Anatomía, Histología y Neurociencia, Facultad de Medicina, Universidad Autónoma de Madrid, Madrid, Spain

Author Copy

Abstract

Type 2 diabetes has a complex pathology that involves a chronic inflammatory state. Emerging evidence suggests a link between the innate immune system receptor NOD1 (nucleotide-binding and oligomerization domain 1) and the pathogenesis of diabetes, in monocytes and hepatic and adipose tissues. The aim of the present study was to assess the role of NOD1 in the progression of diabetic cardiomyopathy. We have measured NOD1 protein in cardiac tissue from Type 2 diabetic (*db*) mice. Heart and isolated cardiomyocytes from *db* mice revealed a significant increase in NOD1, together with an up-regulation of nuclear factor κB (NF-κB) and increased apoptosis. Heart tissue also exhibited an enhanced expression of pro-inflammatory cytokines. Selective NOD1 activation with C_{12}-γ-D-glutamyl-*m*-diaminopimelic acid (iEDAP) resulted in an increased NF-κB activation and apoptosis, demonstrating the involvement of NOD1 both in wild-type and *db* mice. Moreover, HL-1 cardiomyocytes exposed to elevated concentrations of glucose plus palmitate displayed an enhanced NF-κB activity and apoptotic profile, which was prevented by silencing of NOD1 expression. To address this issue in human pathology, NOD1 expression was evaluated in myocardium obtained from patients with Type 2 diabetes (T2DMH) and from normoglycaemic individuals without cardiovascular histories (NH). We have found that NOD1 was expressed in both NH and T2DMH; however, NOD1 expression was significantly pronounced in T2DMH. Furthermore, both the pro-inflammatory cytokine tumour necrosis factor α (TNF-α) and the apoptosis mediator caspase-3 were up-regulated in T2DMH samples. Taken together, our results define an active role for NOD1 in the heightened inflammatory environment associated with both experimental and human diabetic cardiac disease.

Key words: apoptosis, cardiomyocyte, human myocardium, inflammation, nucleotide-binding and oligomerization domain 1 (NOD1), Type 2 diabetes

INTRODUCTION

Diabetes mellitus is the world's fastest growing disease with high rates of morbidity and mortality. A significant number of diabetic patients develop cardiomyopathy, mainly by presenting left ventricular dysfunction independent of coronary artery disease or hypertension. Diabetes is characterized by deregulated lipid metabolism, insulin resistance, mitochondrial dysfunction and disturbances in adipokine secretion and signalling [1]. Myocyte loss and development of fibrosis contribute to the cardiac dysfunction observed in diabetic patients [1,2]. In addition, diabetes is associated with a chronic inflammatory state characterized by increased release of pro-inflammatory mediators [3–5]. In this context, activation of the innate immune system not only mediates the host response against pathogens, but can also contribute to insulin resistance and diabetes progression [6–9]. Accordingly,

Abbreviations: CARD, caspase recruitment domain; COX2, cyclo-oxygenase 2; *db* mouse, Type 2 diabetic mouse; H&E, haemotoxylin and eosin; HFD, high-fat diet; IκB, inhibitor of nuclear factor κB; IKK, inhibitor of nuclear factor κB kinase; iEDAP, γ-D-glutamyl-*m*-diaminopimelic acid; IL, interleukin; NF-κB, nuclear factor κB; NH, normoglycaemic individual(s) without a cardiovascular history; NLR, nucleotide-binding and oligomerization domain-like receptor; NOD1, nucleotide-binding and oligomerization domain 1; NOS2, NO synthase 2; RIP2, receptor-interacting protein 2; T2DMH, patient(s) with Type 2 diabetes; TLR, Toll-like receptor; TNF-α, tumour necrosis factor α; TUNEL, terminal deoxynucleotidyltransferase-mediated dUTP nick-end labelling; wt mouse, wild-type mouse; X-IAP, X-linked inhibitor of apoptosis.

[1]**These authors contributed equally to the study.**

Correspondence: Dr María Fernández-Velasco (email mvelasco@iib.uam.es or maria.fernandez@idipaz.es) or Professor Lisardo Boscá (email lbosca@iib.uam.es).

Clinical Science www.clinsci.org

© The Authors Journal compilation © 2014 Biochemical Society

an increase of innate immune mediators such as Toll-like receptors (TLRs) has been detected in monocytes isolated from Type 2 diabetic patients [10].

In addition to TLRs, the innate response includes a family of cytoplasmic receptors that recognize components of microorganisms or abnormal/damaged host cells: the nucleotide-binding and oligomerization domain-like receptors (NLRs) [11]. Currently, 22 members of the NLR family have been identified in humans [12–14]. Nucleotide and oligomerization domain 1 (NOD1) is an NLR subfamily member that, upon activation, undergoes a conformational modification that allows the recruitment and activation of the protein serine-threonine kinase 2 [receptor-interacting protein 2 (RIP2)], resulting in nuclear factor κB (NF-κB) activation and initiation of inflammatory gene transcription. Dysregulation of NLR function has been described in various diseases, including chronic inflammation, autoimmunity and cancer pre-disposition [14,15]. Activation of NOD1 signalling has been related to the progression of vascular inflammation [16–19] and also to apoptosis [20,21]. Less information is available on the role of NLR signalling in cardiac tissue; however, we have reported previously that NOD1 is expressed in the mouse heart, and NOD1 activation with the selective agonist C_{12}-γ-D-glutamyl-*m*-diaminopimelic acid (referred to subsequently as iEDAP) induces cardiac fibrosis and apoptosis, and also impairs cardiac function [22].

Interestingly, NOD1 has been detected in tissues involved directly in glucose homoeostasis, such as liver, muscle and adipose tissue [23]. Indeed, NOD1 agonists induce insulin resistance both '*in vivo*' and '*in vitro*' through alterations in glucose production and clearance [7,24]. Recently, Shiny et al. [25] demonstrated that monocytes obtained from patients with Type 2 diabetes (T2DMH) have increased mRNA levels of NOD genes. To date, no data are available concerning the role of NOD1 in the inflammatory response in cardiac diseases, including those related to diabetes. Thus, the objective of the present work was to assess the participation of NOD1 in cardiac inflammation linked to diabetes. On this basis, we have determined NLR expression in hearts from *db/db* mice (subsequently referred to as *db*), a rodent model for Type 2 diabetes. Moreover, to gain insight into human pathophysiology of diabetes, we have assessed the presence of NOD1 in cardiac tissue from T2DMH and in myocardium of normoglycaemic individuals without cardiovascular histories (NHs). Our results indicate that the NOD1 pathway is up-regulated in myocardium in both experimental and human diabetes and is associated with an increased pro-inflammatory and apoptosis profile. Thus, NOD1 activation in the heart establishes a new paradigm for linking NLRs to cardiac inflammation related to Type 2 diabetes.

MATERIALS AND METHODS

Ethics

All experiments on humans and mice were performed with the approval of the Consejo Superior de Investigaciones Científicas (CSIC) and the La Paz Hospital human ethics and animal policy and welfare (Ref. DGG28079-37-A) following recommendations of the Spanish and European guidelines (2010/63/EU).

Animal model

The leptin-receptor-deficient *db* mice were used as a rodent model for obesity and Type 2 diabetes; *db*/+ (subsequently referred to as wt) mice were used as a wild-type group.

Chemicals

iEDAP was from InvivoGen and was used to selectively activate NOD1. Staurosporine was purchased from Calbiochem.

Cell isolation

Ventricular cardiomyocytes were isolated from control (wt) and diabetic (*db*) mice using a standard enzymatic digestion as described previously [26].

HL-1 culture

HL-1 cells were seeded in a fibronectin/gelatin (1 mg/ml and 0.02%) coating matrix. Cells were maintained with Claycomb medium (A.T.C.C.) supplemented with 10% FBS, 2 mmol/l L-glutamine, 0.1 mmol/l noradrenaline and 1% penicillin/streptomycin. Cells were grown at 37 °C in an atmosphere of 5% CO_2. Glucose plus palmitate supplementation was added to 1% of acid-free BSA fraction V in Claycomb medium.

NOD1 siRNA silencing

A specific siRNA (sense: 5′-CCGUCUCACGGUUAUCAGAtt-3′; antisense: 5′-UCUGAUAACCGUGAGACGGct-3′; Ambion) was used to silence the expression of the NOD1 gene; an equivalent scrambled sequence served as a control. HL-1 cells were transfected with 100 nM of siRNA using Lipofectamine™ 2000 (Invitrogen). The degree of NOD1 knockdown was determined by a fluorescein conjugate control of siRNA and by Western blot analysis at 24 h and 48 h after transfection. The transfection efficiency of the siRNAs was 70–80%. Transfection with a scrambled siRNA did not modify the NOD1 levels in vehicle and glucose plus palmitate-treated cells.

Glucose and palmitate supplementation and drug treatment

Palmitate stock solution was prepared in DMSO. Controls cells were treated with vehicle (BSA and DMSO). Glucose, palmitate and actinomycin D were from Sigma.

Preparation of total protein cell extracts

Tissues/cells were homogenized using a handheld blender in lysis buffer [50 mmol/l Tris/HCl (pH 7.0), 320 mmol/l sucrose and 1 mmol/l DTT plus a complete protease and phosphatase inhibitor solution (Sigma)]. The homogenate was centrifuged at 13 000 ***g*** for 10 min at 4 °C, and supernatants were frozen and stored at − 80 °C for Western blot analysis. Protein concentrations were determined by the Bradford assay (Bio-Rad).

Preparation of nuclear and cytosolic protein extracts for p65 analysis

Cardiac tissue was homogenized by 10 s sonication at 4 °C in homogenization cytosolic buffer [10 mmol/l Hepes (pH 8),

Author Copy

 © The Authors Journal compilation © 2014 Biochemical Society

10 mmol/l KCl, 1 mmol/l EDTA, 1 mmol/l EGTA and 0.5% Nonidet P40]. Tissue pieces were vortex-mixed and centrifuged at 12 000 ***g*** for 30 min. Supernatant was taken as the cytosolic fraction. The pellet was re-suspended in 50 μl of ice-cold nuclear buffer [20 mmol/l Hepes (pH 8), 0.4 mmol/l NaCl, 1 mmol/l EDTA, 1 mmol/l EGTA and 20% glycerol] and vortex-mixed at 4 °C for 30 min. After centrifugation (12 000 ***g*** at 4 °C for 20 min), the supernatant (nuclear fraction) was collected. All buffers contained a protease and phosphatase inhibitor cocktail (Sigma).

Western blot analysis

Equal amounts of protein (20–80 μg) were separated by SDS/PAGE (10–12% gel). Proteins were size fractionated, transferred on to a Hybond-P membrane (GE Healthcare) and, after blocking with 5% non-fat dry milk, incubated with the corresponding antibodies. The blots were developed by the ECL protocol (GE Healthcare), and different exposure times were performed for each blot with a charge-coupled device camera in a luminescent image analyser (Molecular Imager, Bio-Rad) to ensure the linearity of the band intensities. Values of densitometry were determined using Quantity One software (Bio-Rad). Antibodies against NOD1, phospho-RIP2, RIP2, phospho-IKK (inhibitor of nuclear factor κB kinase), IKK, phospho-IκBα (inhibitor of nuclear factor κB α), IκBα, NOS2 (NO synthase 2), COX2 (cyclo-oxygenase 2), p65, caspase-3, BAX and X-IAP (X-linked inhibitor of apoptosis) were purchased from the Santa Cruz Biotechnology or the Cell Signaling Technology. An anti-[human NOD1 (hNOD1)] antibody was purchased from R&D Systems.

RNA isolation and reverse transcription–PCR

RNA was extracted from cells using TRI Reagent® solution (Ambion) and 1 μg was reverse-transcribed into cDNA using the Transcriptor first strand cDNA synthesis kit (Roche). Then, real-time PCR was performed with this template cDNA adding FastStart Universal SYBR Green Master (Roche) and the specific primers in a MyIQ thermocycler (Bio-Rad). Each sample was run in duplicate and was normalized to 18S RNA. The replicates were then averaged and fold induction was determined by $\Delta\Delta C_t$-based fold-change calculations. Primers sequence were the following tumour necrosis factor α (TNF-α) forward: 5′-CATCTTCTCAAAATTCGAGTGACAA-3′; reverse: 5′-TGGGAGTAGACAAGGTACAACCC-3′; IL (interleukin)-1β forward: 5′-GAAGCTGTGGCAGCTACCTG-3′; reverse: 5′-GAAAAGAAGGTGCTCATGTCC-3′; IL-6 forward: 5′-CTGCAAGAGACTTCCATCCAGTT-3′; reverse: 5′-GAAGTAGGGAAGGCCGTGG-3′; 18S forward: 5′-GCAATTATTCCCCATGAACGA-3′; reverse: 5′-AAAGGGAGGGACTTAATCAA-3′.

Cell death and viability detection

For detection and quantification of apoptosis, the terminal deoxynucleotidyltransferase-mediated dUTP nick-end labelling (TUNEL) commercial kit for cell death detection (Roche) was used. The cell survival assay relies on the capacity of cells to reduce MTT (Calbiochem) to a coloured formazan in metabolically active cells. Cardiomyocytes from both wt and *db* mice suspended in storage solution were incubated for 2 h with 0.5 mg/ml MTT in the dark at 37 °C, and then 100 μl of 50% dimethylformamide in 20% SDS (pH 4.7) was added. Absorbance was measured at 595 nm. All assays were performed in triplicate.

Table 1 Comparison of the biochemical data from human subjects

HbA_{1c}, glycated haemoglobin; HDL, high-density lipoprotein; LDL, low-density lipoprotein; ns, not significant.

Parameter	NH ($n=5$)	T2DMH ($n=6$)	*P* value
Age (years)	41.4 ± 7.8	72 ± 2.3	$P<0.01$
Weight (kg)	71.2 ± 3.3	81.9 ± 16.9	ns
Glucose (mg/dl)	84.5 ± 3.2	164.6 ± 20.5	$P<0.01$
HDL-cholesterol (mg/dl)	54.5 ± 2.0	30.2 ± 3.8	$P<0.01$
LDL-cholesterol (mg/dl)	111.7 ± 1.2	163.2 ± 45.5	ns
LDL/HDL-cholesterol ratio	2.7 ± 0.4	4.1 ± 0.6	$P<0.05$
HbA_{1c} (%)	4.4 ± 0.1	6.9 ± 0.7	$P<0.05$

Human specimens

Myocardial samples from six T2DMH and five NH were obtained during autopsy procedure at the La Paz Hospital. Human cardiac samples were taken during the forensic autopsy (post-mortem time <48 h). Post-mortem time was defined as the estimated time from death to autopsy. Cardiac tissues were processed rapidly to avoid possible deleterious changes at the cellular level. Full informed written consent was obtained from the family of all donors. Biochemical data of all subjects are included in Table 1. Gross and histopathological study of hearts from NH and T2DMH did not show any acute myocardial lesions. For histopathological procedures, tissues were processed by fixing in 4% buffered formalin and embedded in paraffin wax. The diabetic complications registered in the autopsy history included a patient who suffered an ictus and other individual who had acute kidney failure.

Immunohistochemistry

Serial 5-μm-thick transverse sections of left ventricular cardiac tissue were mounted on glass slides and allowed to dry. Sections were stained with haemotoxylin and eosin (H&E) or deparaffinized, unmasked and peroxidase-blocked by incubating in 0.1% H_2O_2 diluted in methanol, blocked in 1% BSA and 5% NGS (normal goat serum) in TBS for 2 h and then exposed to anti-NOD1 (1:100 dilution; R&D Systems), -TNF-α (1:400 dilution; Abcam) or -caspase-3 (1:100 dilution; Cell Signaling) antibody overnight at 4 °C. Antibodies were labelled with a biotinylated streptavidin-biotin method and visualized with diaminobenzidine. Slides were then counter-stained with haematoxylin before being dehydrated, cleared and mounted. Photographs were taken with a microscope (Olympus CX40).

Statistics

Data are presented as means ± S.E.M. Statistical significance was assessed using a Student's *t* test or ANOVA, followed by the

Author Copy

Bonferroni's test when appropriate. Differences with values of $P < 0.05$ were considered statistically significant.

RESULTS

Expression of NOD1 in the myocardium of diabetic mice

As previous evidence suggests that NOD1 can participate in diabetes [7,27–29], we have evaluated the expression of NOD1 in the myocardium of a transgenic *db* mouse model. *db* mice manifest several indicators common to patients with Type 2 diabetes, including obesity, hyperglycaemia, hyperinsulinaemia and depressed cardiac function [30–33]. Accordingly, *db* mice were significantly heavier than their wt counterparts and had increased blood concentrations of glucose and insulin (Supplementary Figure S1 at http://www.clinsci.org/cs/127/cs1270665add.htm). NOD1 protein expression, detected by Western blot analysis, was found in cardiac tissue from both *db* mice and corresponding wt mice; however, expression was significantly greater in *db* mice (Figure 1A, $P < 0.01$ compared with wt mice). Together with elevated NOD1 levels, cardiac tissue from *db* mice also exhibited an increase in the phosphorylation of the NOD1 adapter RIP2 that leads to NF-κB activation [34], demonstrated by increased levels of phospho-IKK/IKK and phospho-IκBα/IκBα (Figure 1A) and nuclear enrichment of p65 (Figure 1A, right panel). Interestingly, hearts from *db* mice also contained elevated levels of NOS2 and COX2, consistent with NF-κB activation (Figure 1B). These changes were also accompanied by significant increases in the levels of the pro-inflammatory cytokines TNF-α, IL-6 and IL-1β in hearts from *db* mice relative to wt mice (Figure 1B).

To validate these results in a second diabetes model, we have determined NOD1 expression in cardiac tissue from mice subjected to a high-fat diet (HFD) to provoke obesity. Predictably, mice fed on the HFD for 12 weeks were significantly heavier than chow-fed littermates and had significantly greater levels of serum glucose and insulin (Supplementary Figure S2 at http://www.clinsci.org/cs/127/cs1270665add.htm). Notably, HFD-fed mice also demonstrated increased expression of NOD1 in heart tissue compared with chow-fed littermates (Supplementary Figure S2). Thus, in two independent models of hyperglycaemia, NOD1 protein is elevated in cardiac tissue.

Given that cardiac apoptosis participates in the pathogenesis of diabetes [2], and a direct relationship between NOD1 activation and apoptosis induction has been previously established [20,21], we next questioned whether NOD1 activation was responsible for cardiomyocyte apoptosis. Thus, TUNEL assays were performed on cardiac tissue, and we have measured activated caspase-3, X-IAP and BAX protein in *db* and wt mice. In contrast with tissue from wt mice, ventricular tissue from *db* mice contained higher levels of the pro-apoptotic proteins caspase-3 and BAX and lower levels of the anti-apoptotic mediator X-IAP (Figure 1C). A similar result was obtained by TUNEL staining (Figure 1D), showing a greater degree of DNA fragmentation in cardiac tissue from *db* mice (7.7 ± 4.1 % of TUNEL-positive cells in *db* mice compared with 0.9 ± 1.0 % in wt mice).

Cardiomyocytes isolated from hearts of *db* mice exhibit NOD1 activation and increased apoptosis

To assess whether the pathological changes observed in the hearts of *db* mice were related to changes at the level of the cardiomyocyte, we have isolated cardiomyocytes from hearts of *db* and wt mice and analysed the expression of NOD1. Immunostaining of cardiomyocytes from wt and *db* mice revealed intense NOD1 reactivity in cardiomyocytes from *db* mice and reduced staining in cells from wt mice (Figure 2A). Similarly, Western blot analysis demonstrated a 3-fold increase in NOD1 expression in cardiomyocytes from *db* mice relative to controls (Figure 2B). In addition, NF-κB activation and expression of the COX2 target gene was also significantly greater in cardiomyocytes isolated from hearts of *db* mice (Figure 2B). Furthermore, cardiomyocytes isolated from hearts of *db* mice were more apoptotic, measured as the number of TUNEL-positive cells (Figure 2C), and their viability was reduced, as determined by an MTT assay (Figure 2D). Consequently, cardiomyocytes from *db* mice had greater levels of the pro-apoptotic proteins caspase-3 and BAX, together with reduced levels of the anti-apoptotic protein X-IAP (Figure 2E). Finally, to assess whether cardiomyocytes from *db* mice were more sensitive to cell death/apoptosis, we have treated cardiomyocytes from both *db* and wt mice with the alkaloid staurosporine to induce apoptosis. Interestingly, staurosporine-induced apoptosis was maximal in cells isolated from hearts of *db* mice, and they also exhibited the greatest loss in cell viability (Supplementary Figure S3 at http://www.clinsci.org/cs/127/cs1270665add.htm).

Selective stimulation of NOD1 induces activation of NF-κB and apoptosis

Given the results described above, we next investigated whether specific activation of NOD1 would lead to a similar inflammatory profile and activation of apoptosis in mice. To do this, we have taken advantage of the selective NOD1 agonist iEDAP [35,36]. wt and *db* mice were treated daily with an intraperitoneal injection of iEDAP (5 μg/g of body weight), or vehicle, over a 2-week period, and hearts were examined for activation of NOD1. Western blot analysis of heart tissue demonstrated that, compared with control mice, wt mice injected with iEDAP exhibited a statistically significant increase in both phospho-IKK/IKK and phospho-IκBα/IκBα expression and the NF-κB target genes NOS2 and COX2 (Supplementary Figure S4A at http://www.clinsci.org/cs/127/cs1270665add.htm) to levels comparable with those found in *db* mice. In addition, iEDAP treatment of *db* mice further increased the expression of these inflammatory markers (Supplementary Figure S4A). As anticipated, analysis of TUNEL-positive nuclei in treated and non-treated mice revealed that NOD1 activation by iEDAP increased the number of apoptotic cells in heart tissue compared with vehicle-treated animals (Supplementary Figure S4B). This was accentuated in iEDAP-treated *db* mice. Finally, analysis of pro-apoptotic protein expression mirrored the TUNEL analysis (Supplementary Figure S4C) and showed that iEDAP treatment up-regulates caspase-3 and BAX, while reducing X-IAP. Collectively, these results reinforce our findings in *db* mice and indicate that NOD1 stimulation is associated with increased apoptosis and inflammatory gene activation.

Author Copy

 © The Authors Journal compilation © 2014 Biochemical Society

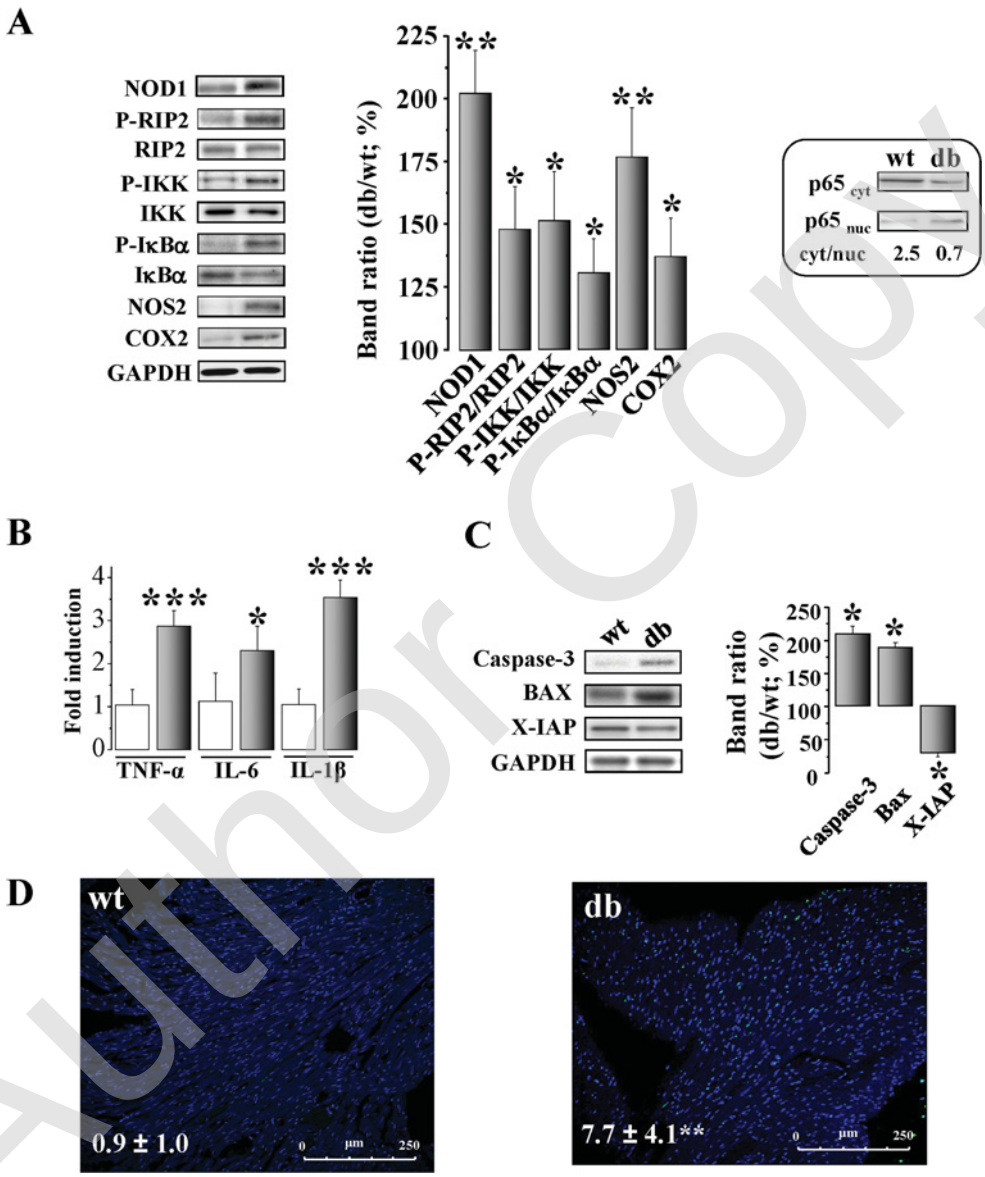

Figure 1 **Cardiac expression of NOD1, NF-κB and apoptotic pathways are enhanced in *db* mice**

(**A**) Left panel shows representative immunoblots of NOD1, phospho-RIP2, RIP2, phospho-IKK, IKK, phospho-IκBα, NOS2 and COX2 in hearts from wt and *db* mice. Glyceraldehyde-3-phosphate dehydrogenase (GAPDH) was used for normalization. Central panel shows histograms representing the mean ± S.E.M. values, expressed as a percentage compared with wt mice (100 %); $n = 4$–6 animals. Right panel shows a representative example of p65 distribution in cytosolic and nuclear fractions in the wt and *db* groups. (**B**) Fold induction of cardiac expression of TNF-α, IL-6 and IL-1β in hearts from *db* mice (shaded) relative to wt mice (white). (**C**) Left panel shows representative immunoblots of activated caspase-3, BAX and X-IAP obtained from heart tissue of wt and *db* mice and the corresponding densitometry (right panel, $n = 4$). GAPDH was used for normalization of loading. (**D**) Representative images of TUNEL (green) and DAPI (blue) staining in cardiac tissue sections of *db* and wt mice (×40, 5 µm/slide). Mean ± S.E.M. values of TUNEL-positive cells have been added to the images. Light transmission of TUNEL preparations point to cardiomyocytes as the main apoptotic phenotype involved. Data are expressed as means ± S.E.M. compared with wt mice (100 %). $^{*}P < 0.05$, $^{**}P < 0.01$ and $^{***}P < 0.001$ compared with wt mice.

High concentrations of palmitate and glucose induce the up-regulation of NOD1 and apoptotic signalling in HL-1 cells

In an attempt to mimic the diabetes-like pathological micro-environment found *in vivo*, we have used the HL-1 cardiomyocyte cell line, exposed these cells to high concentrations of glucose plus palmitate (lipid-induced insulin resistance model) for 48 h and assessed changes to the NOD1 signalling pathway. As expected, exposure of HL-1 cells to glucose plus palmitate resulted in lipid accumulation together with

Author Copy

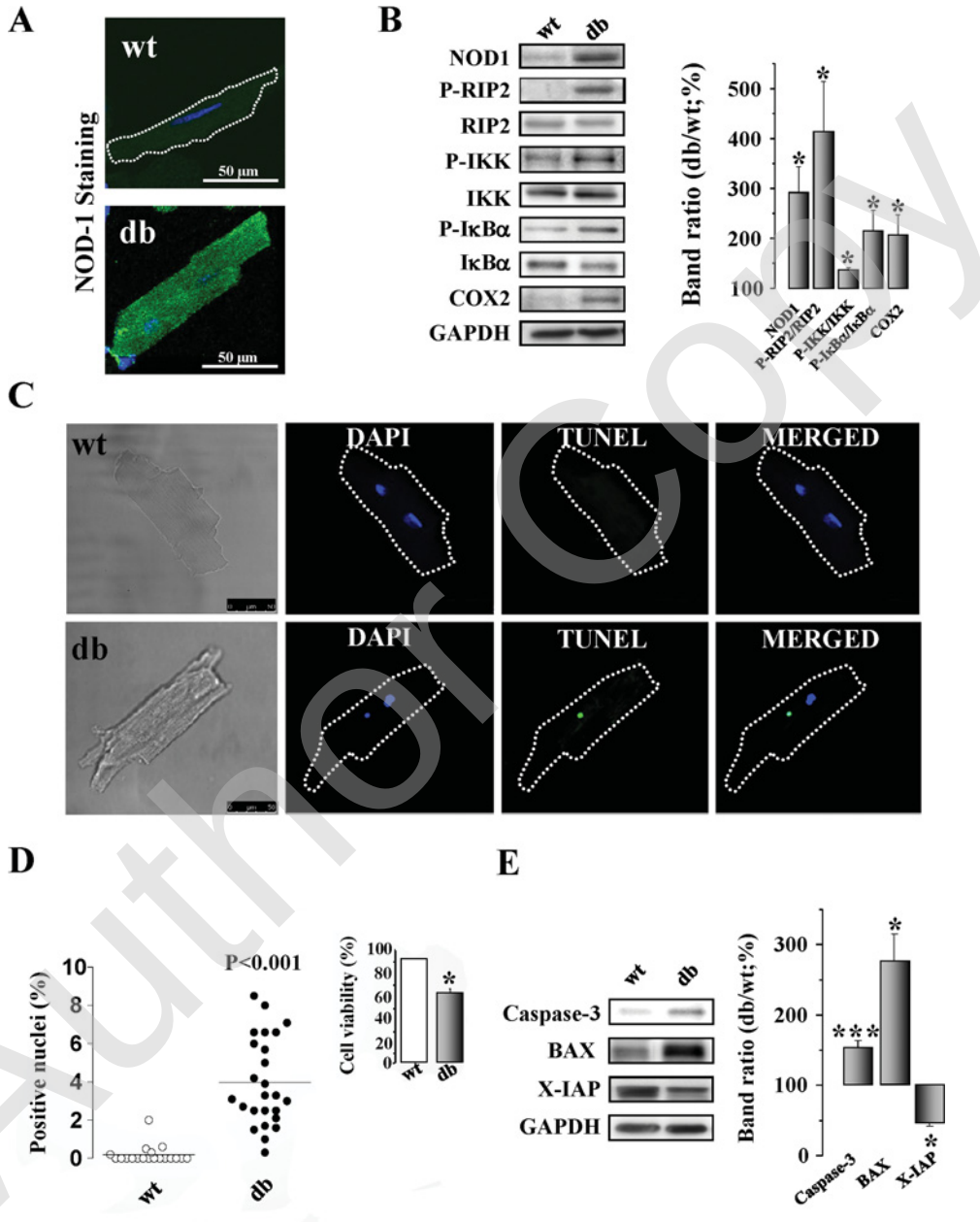

Figure 2 Cardiomyocytes isolated from *db* mice overexpress NOD1 and exhibit sustained activation of NF-κB and apoptosis pathways

(**A**) Confocal microscopy images of a representative cardiomyocyte isolated from the heart of a wt and *db* mouse stained for NOD1. (**B**) Immunoblot analysis of NOD1 signalling. Left panel shows representative blots of NOD1, phospho-RIP2/RIP2, phospho-IKK/IKK, phospho-IκBα/IκBα and COX2 from isolated cardiomyocytes of wt and *db* mice. Right panel shows the means ± S.E.M. ($n = 4$ cell preparations) expressed as a percentage compared with wt mice (100 %). (**C**) Representative TUNEL assay of cardiomyocytes from wt and *db* mice (green staining is TUNEL positive nuclei; blue corresponds to DAPI nuclei staining). Means ± S.E.M. are represented in (**D**); right panel shows cell viability measured by MTT ($n = 4$–6 assays per condition). (**E**) Representative immunoblots of activated caspase-3, BAX and X-IAP in isolated cardiomyocytes from hearts of wt and *db* mice. Means ± S.E.M. are expressed as a percentage of wt mice (100 %).*$P < 0.05$ and ***$P < 0.001$ compared with wt mice ($n = 4$ cell preparations).

impairment of insulin signalling (Supplementary Figure S5 at http://www.clinsci.org/cs/127/cs1270665add.htm). In addition, HL-1 cells treated with glucose and palmitate showed increased expression of NOD1, as measured by immunofluorescence (Figure 3A) and Western blot analysis (Figure 3B). Moreover, RIP2 phosphorylation and NOS2 induction were increased similarly upon treatment (Figure 3B). Notably, siRNA silencing of NOD1 decreased the activation of downstream targets, including RIP2 and NOS2, in HL-1 cells exposed to glucose and palmitate (Figure 3B). Importantly, exposure of HL-1 cardiomyocytes

 © The Authors Journal compilation © 2014 Biochemical Society

separately to glucose or palmitate failed to induce changes in NOD1 expression (results not shown). The addition of glucose plus palmitate to HL-1 cells also promoted the activation of pro-apoptotic pathways, increasing activated caspase-3 and decreasing the anti-apoptotic protein X-IAP (Figure 3C). Significantly, activation of apoptosis was prevented in cardiomyocytes silenced for NOD1 expression (Figure 3C). Importantly, NOD1 silencing did not affect pro-inflammatory and pro-apoptotic pathways under basal conditions (results not shown). To determine whether high glucose/fatty acid treatment up-regulated NOD1 at the transcriptional level, we have treated HL-1 cells as before together with a selective inhibitor of transcription (actinomycin D). Results revealed that the addition of actinomycin D prevented NOD1 up-regulation induced by the high glucose/fatty acids administration (Figure 3D), demonstrating that the increase in NOD1 expression occurs at the level of transcription.

NOD1 is overexpressed in the myocardium of diabetic patients

Having demonstrated the activation of NOD1 in diabetic murine myocardium, we next sought to identify whether a similar situation occurred in human pathology. To this end, we have measured NOD1 protein expression in myocardium samples of left ventricle from T2DMH and NH. Table 1 gives the human biochemical data from the patients. Representative immunohistochemistry images of NOD1 expression in a sample from an NH and T2DMH are shown in Figure 4. Transversal sections were stained with H&E to distinguish the underlying histology (Figures 4a and 4b). NOD1 expression was marked significantly in both transversal (Figures 4c and 4d) and longitudinal (Figures 4e and 4f) sections of T2DMH compared with NH. Importantly, no background staining was observed when using only the secondary antibody (Supplementary Figure S6 at http://www.clinsci.org/cs/127/cs1270665add.htm). In addition, immunofluorescence analysis showed that NOD1 protein expression in T2DMH was increased significantly (1.9 ± 0.1 arbitrary units in T2DMH compared with 1.1 ± 0.1 arbitrary units in NH; $P < 0.01$; Supplementary Figure S7 at http://www.clinsci.org/cs/127/cs1270665add.htm). Consistent with our *in vitro* experiments, immunohistochemical analysis suggested NOD1 overexpression in the cardiomyocyte population, defined as easily identifiable rod-shaped cells in longitudinal sections (Figures 4e and 4f, and Supplementary Figure S7). Furthermore, sections of hearts from T2DMH showed increased staining for the pro-inflammatory cytokine TNF-α (Figure 5A) together with a higher percentage of cells stained positively for caspase-3, compared with sections of hearts from NH ($1.7 \pm 0.2‰$ of caspase-3-positive cells in T2DMH compared with $0.0 \pm 0.0‰$ found in NH; $P < 0.01$, Figure 5B).

DISCUSSION

In the present report, we have demonstrated that the myocardium from mouse models of diabetes and human myocardium of patients with Type 2 diabetes overexpress the receptor of the innate immune system NOD1. This up-regulation occurred in cardiomyocytes and was associated with an increased apoptotic profile.

During their lifetime, humans are confronted frequently with pathogens. To resolve an infectious process, the innate immune system uses a complex signalling network to modulate the delicate balance between stimulation and inhibition of host immune responses. Imbalances in the innate immunity system promote chronic inflammatory and autoimmune processes that can potentially participate in the onset of several pathologies including diabetes [7,37]. In this context, it has been proposed that some mediators of the innate immune response might contribute to ongoing obesity-associated insulin resistance, indicating a connection between innate immunity and metabolic regulation. Both TLRs and NLRs, the most prominent mediators of the innate immune system, participate in coronary heart disease, myocardial infarction and diabetes [5,8,38–40]. NOD1, a member of the NLR family, has been associated with the induction of chronic inflammatory disorders, such as atopic eczema and asthma [41,42]. These examples underscore the importance of this receptor in the regulation of the immune response [43,44], including NF-κB activation, cytokine production and induction of apoptosis [45,46]. At the vascular level, NOD proteins can mediate several inflammatory responses [16,17]. However, despite the marked progress in understanding the role of NLR/NOD signalling in host defence, their contribution to inflammatory cardiac disorders remains poorly characterized [47].

Recent studies point to a direct relationship between NOD proteins and diabetes. In this respect, some studies have reported that NOD proteins participate in insulin resistance and inflammatory responses in hepatocytes from diabetic mice [7]. Cross-talk between diabetes-related inflammation and NOD1 activity appears to be a relevant physiopathological condition in some target tissues, such as the heart. In addition, other pro-inflammatory mediators have been considered as a bridge between metabolism and the immune system. This is the case with TLRs, which are additional pattern-recognition receptors implicated in insulin resistance. Accordingly, TLR4 has been proposed as an immune receptor that can alter metabolism [9] and can recognize not only exogenous but also endogenous ligands, for example modified low-density lipoprotein (LDL) [38], an established cardiovascular risk factor for Type 2 diabetes linked to obesity.

In the present report, we have demonstrated that cardiac tissue from mice with Type 2 diabetes expresses higher levels of NOD1, together with increased production of pro-inflammatory cytokines including TNF-α, IL-1β and IL-6. Supporting these findings, other studies have described that NOD1 activation promotes insulin resistance in adipocytes and hepatocytes [7,24,27,28]. Moreover, monocytes isolated from patients with Type 2 diabetes have higher expression of NOD1 compared with normoglycaemic individuals [25]. Furthermore, Schertzer et al. [7] have demonstrated in a model of Type 2 diabetes induced by an HFD that the absence of NOD protects against lipid accumulation and insulin resistance. Collectively, these observations support the involvement of NOD1 in metabolic disorders.

Regarding the mechanism responsible for activation of NOD1 in the heart of *db* mice, a plausible explanation might be that NOD1 is activated by fatty acids. This notion is supported by

Author Copy

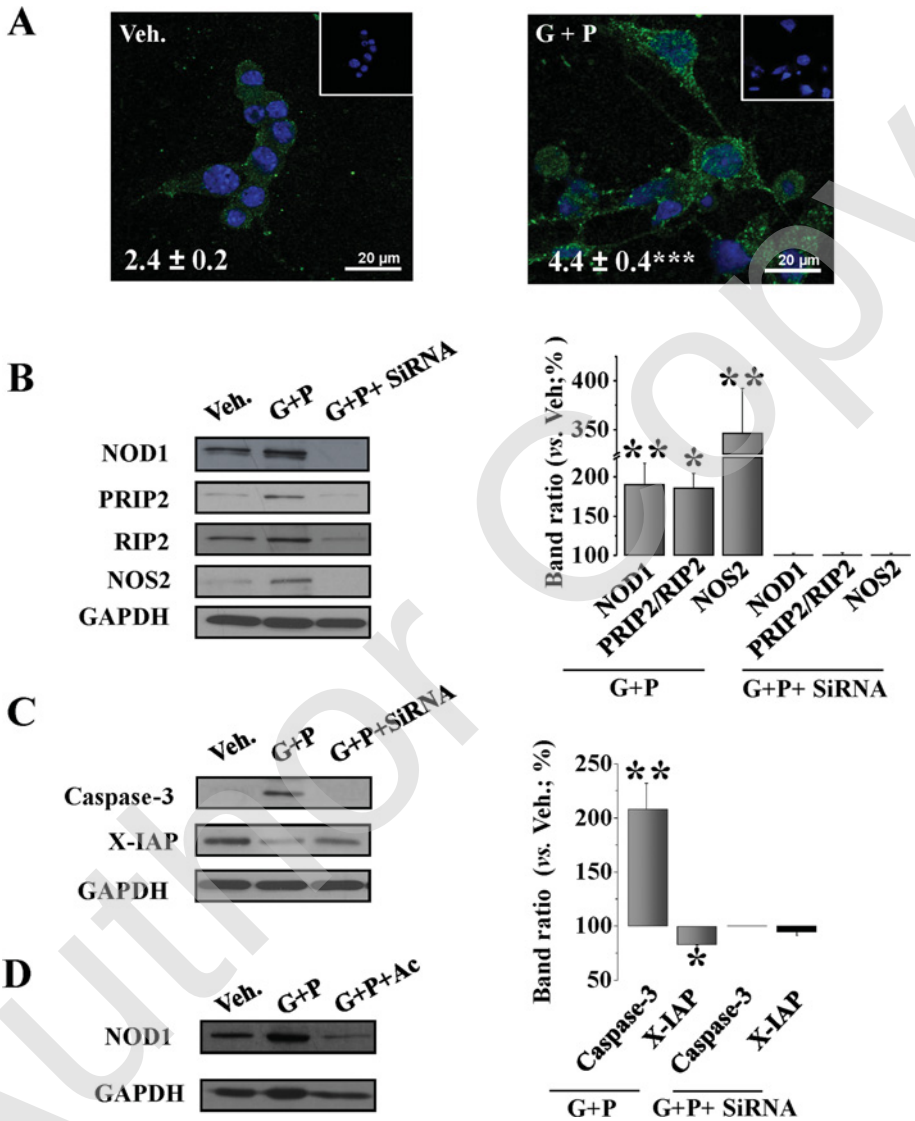

Figure 3 HL-1 cardiomyocytes incubated with high doses of glucose and palmitate promote NOD1 pathway activation and apoptosis induction

(**A**) Representative immunostaining of NOD1 obtained in HL-1 cardiomyocytes incubated 48 h with vehicle (Veh.) or with 50 mmol/l glucose plus 200 μmol/l palmitate (G + P); a negative control of each example is shown in the inset. Mean fluorescence values ± S.E.M. in arbitrary units are inserted in the images. (**B**) Representative blots of NOD1, phospho-RIP2/RIP2 and NOS2 obtained in HL-1 cells treated with Veh., G + P or G + P + siRNA of NOD1 (G + P + siRNA). (**C**) Left panel shows representative blot of activated caspase-3 and X-IAP obtained in Veh., G + P and G + P + siRNA-treated cells. (**D**) Representative blot of three different experiments representing NOD1 expression in HL-1 cells treated with Veh., G + P or G + P + 0.1 μg/ml actinomycin D (G + P + Ac). Means ± S.E.M. ($n = 3$–5) are expressed as a percentage compared with wt mice (100 %). $^{*}P < 0.05$, $^{**}P < 0.01$ and $^{***}P < 0.001$ compared with Veh.

our findings in cardiomyocytes treated with high concentrations of glucose and palmitate. This environment leads to transcriptional up-regulation of NOD1, together with activation of downstream signalling. Importantly, this activation was abrogated by siRNA silencing of NOD1 (Figure 3). Indeed, Zhao et al. [48] showed that increased lipid metabolites, associated with Type 2 diabetes, can be detected by NOD proteins, and, more recently, Cuda et al. [28] described that the Glu266Lys polymorphism in the *NOD1* gene affects the relationship between nutritional saturated fatty acid intake and insulin sensitivity.

Up-regulation of NOD1 oligomerization through its nucleotide-binding domain results in activation of different pathways, of which the best characterized is NF-κB [23]. Our data show that NF-κB is activated in cardiac tissue of *db* mice (Figure 1). The sustained up-regulation of the NOD1/NF-κB axis observed in the hearts of *db* mice correlates with NLR

 © The Authors Journal compilation © 2014 Biochemical Society

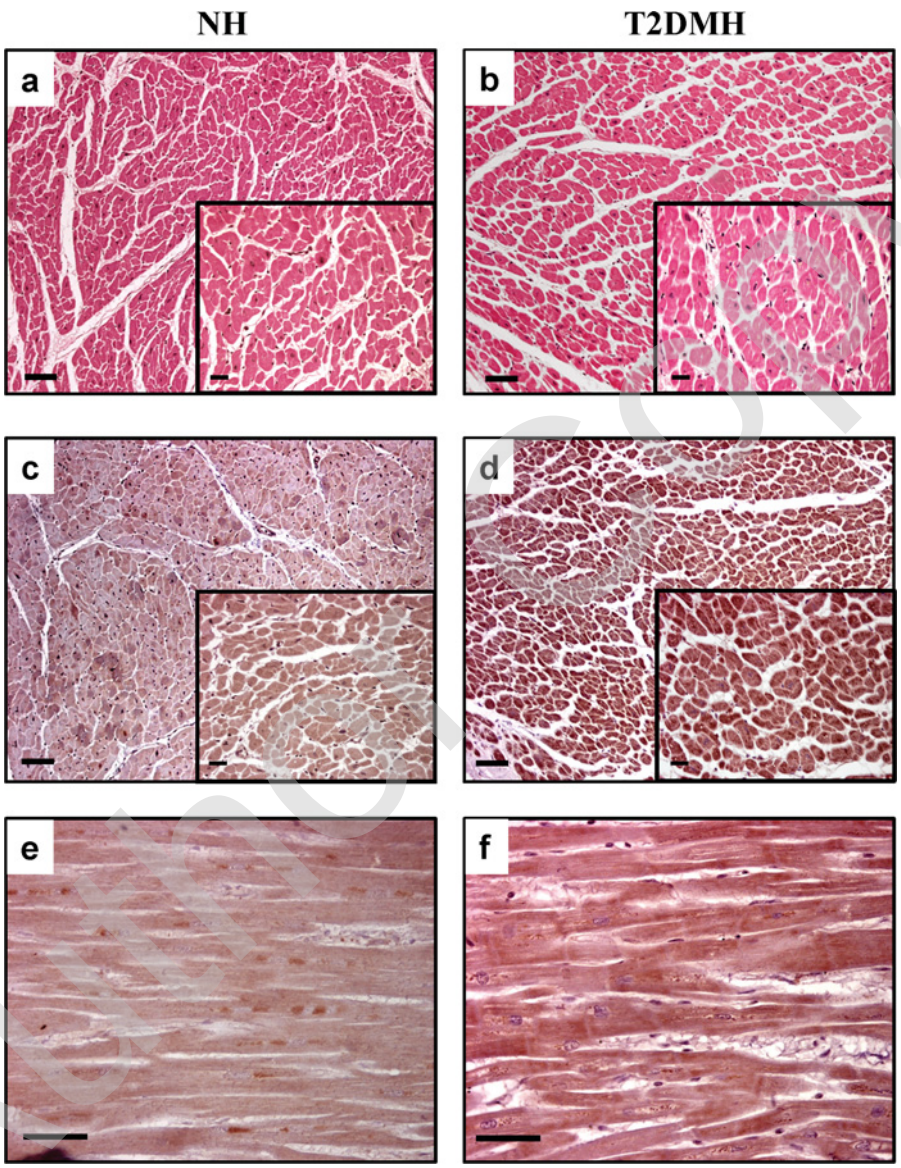

Figure 4 **NOD1 is up-regulated in cardiac tissue from Type 2 diabetic patients**
Representative H&E-stained slides of hearts from NH (**a**) and T2DMH (**b**) (×10). (**c**–**e**) Immunohistochemistry staining demonstrating that NOD1 is overexpressed in both transversal (**c**, **d**, ×10; insert ×40) as well as longitudinal (**e**, **f**, ×40) myocardial sections of hearts from T2DMH relative to NH. Bar = 100 μm.

activation in isolated cells. Thus, our results provide evidence of functional activation of the classical NF-κB pathway, including phosphorylation of IKK, and the expression of target genes such as COX2 and NOS2. NF-κB activation induced by NOD1 is the result of an interaction between the caspase recruitment domain (CARD) of NOD1 and the equivalent CARD of RIP2 [23], a kinase that specifically amplifies downstream signalling from NOD proteins but not from other TLRs [49–51]. The precise function of this kinase is not fully elucidated, but studies with genetic mouse models suggest that RIP2 activity is required for an appropriate innate immune response promoted via NOD receptors [52]. We have demonstrated that RIP2 is activated in both the hearts and cardiomyocytes of *db* mice, corroborating the pathway activation of this NLR in the cardiac milieu in our models.

Apoptotic events have been implicated in the diabetic process [53], although the precise mechanism(s) remain unknown. NLR proteins harbour functions beyond those engaged with the innate immune response, including the regulation of cell death [23,54]. Our previous work established that NOD1 activation induces apoptosis in the heart and in isolated cardiomyocytes [22]. In the present study, we have shown that both cardiac tissue and isolated cardiomyocytes from *db* mice display a prominent pro-apoptotic profile, exhibiting a greater degree of DNA fragmentation compared with wt mice. Furthermore, pro-apoptotic mediators, such as activated caspase-3 and BAX, were increased, whereas cell

Author copy

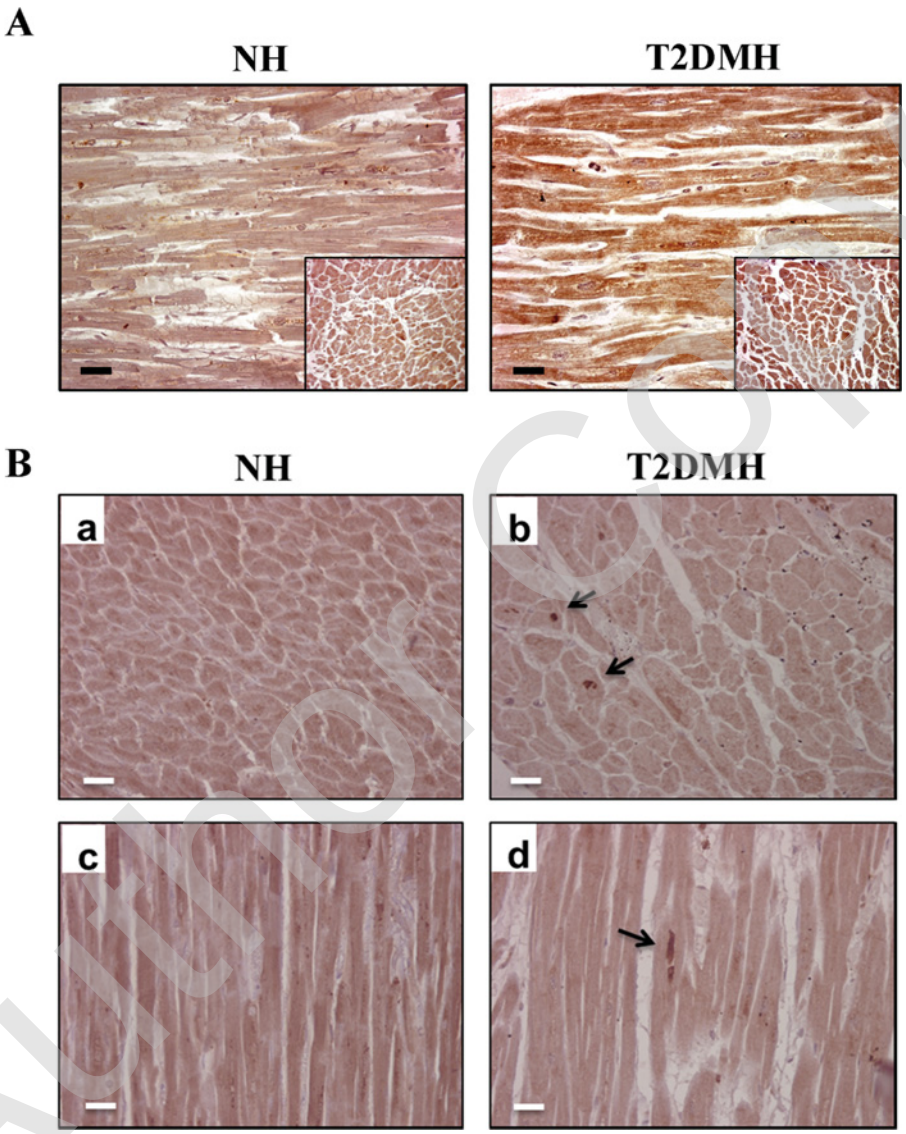

Figure 5 **TNF-α and caspase-3 are up-regulated in myocardium of Type 2 diabetic individuals**
(**A**) Myocardial longitudinal sections of hearts from NH and T2DMH were stained with an antibody to TNF-α (×40); images from transversal sections are inserted in each photomicrograph. (**B**) Myocardial sections from NH and T2DMH were stained with an antibody to caspase-3 (×40). Caspase-3 staining in both transversal (**b**) and longitudinal (**d**) sections of T2DMH shows a high expression of this mediator compared with NH (**a**, **c**).

viability and the anti-apoptotic protein X-IAP were reduced in cardiac tissue and cardiomyocytes from *db* mice. These results were validated in the HL-1 cardiomyocyte cell line. HL-1 cells treated with high concentrations of glucose plus palmitate displayed a pro-apoptotic profile, which was lost upon NOD1 silencing. This relationship between NOD1 activation and caspase-dependent apoptosis is well established by several groups, including ours [20,21,23]. Indeed, the CARD of NLR proteins can interact with the homologous CARD of caspases, triggering an induction of apoptosis. Reinforcing these results, treatment of *db* mice with a selective agonist of NOD1 induces both NF-κB and apoptosis pathways (Supplementary Figure S4), demonstrating the sensitivity of the *db* model to apoptosis induction by specific NOD1 stimulation.

In an attempt to connect our murine data to human pathology, we have analysed NOD1 protein in cardiac tissue from T2DMH and NH. Immunohistochemistry and immunofluorescence demonstrated that T2DMH samples exhibited greater NOD1 expression than NH; this increase was detected notably in cardiomyocytes. Furthermore, levels of the pro-inflammatory cytokine TNF-α were also enhanced in T2DMH compared with NH. Finally, consistent with our results, in the *db* mice model, the

Author Copy

 © The Authors Journal compilation © 2014 Biochemical Society

T2DMH group also showed increased levels of the pro-apoptotic mediator caspase-3. To the best of our knowledge, this is the first demonstration of NLR activity in the human heart. In this context, other mediators of the innate immune system, such as TLR4, are increased in human failing myocardium [55], supporting the idea of cross-talk between innate immune mediators and cardiovascular disease.

During the last decade, the role of the inflammatory response during the onset of diabetes and potential inhibition of inflammatory mediators as alternative or complementary strategies for the management of this disease has received increased attention [56]. Moreover, some evidence supports the idea that chronic inflammation can be a consequence of an inability to shut down the inflammatory response. This is supported by studies demonstrating spontaneous inflammatory events in patients and animals with particular mutated or disrupted genes. Importantly, some of these genes encode proteins which are known to be highly pro-inflammatory, such as the transcription factor NF-κB, emphasizing the complexity of immune regulation. Although further studies will be required to address the specific role of NOD1 in diabetic cardiomyopathy, the present report uncovers a new immune player in the heightened inflammatory response in both human and murine diabetic diseases.

CLINICAL PERSPECTIVES

- NOD1 activity is associated with many pro-inflammatory conditions; however, little is known regarding its contribution to cardiovascular pathologies.
- Our data in animal models and in patients provide strong evidence for an association between Type 2 diabetes and overexpression of NOD1 in cardiac tissue. In addition, we have provided functional evidence, which links the up-regulation of NOD1 to its activation and contribution to chronic low-grade inflammation in the heart.
- Inhibitors of NOD1 are potential therapeutics for diseases with an inflammatory component. The present study identifies relevant targets to assess their potential efficacy in the management of cardiac dysfunction in Type 2 diabetes. Unravelling the therapeutic value of pharmacological inhibitors of NOD1 might provide additional tools for the assessment of cardiac dysfunction associated with up-regulation of NOD1.

AUTHOR CONTRIBUTION

María Vallejo Cremades and Gemma Benito contributed equally to the manuscript. María Fernández-Velasco and Lisardo Boscá conceived and designed the experiments. Patricia Prieto, María Vallejo-Cremades, Gemma Benito, Pilar González-Peramato, Daniel Francés, Javier Regadera, Verónica Terrón, Ivette Pacheco, Noelia Agra and Silvia Gónzalez-Ramos performed the experiments. Patricia Prieto, Javier Regadera, María Vallejo-Cremades and Gemma Benito analysed the data. Mariano Ruiz-Gayo, Carmen Delgado, Juan Velasco-Martín, Paloma Martín-Sanz and Eduardo López-Collazo contributed reagents, materials and analysis tools. María Fernández-Velasco and Lisardo Boscá wrote the paper.

ACKNOWLEDGEMENTS

We thank Dr AM Gómez and Dr L Pereira (INSERM U-637) for sharing samples in the preliminary analysis. We thank the technical assistance of Maria J. Guillén, Diego Navarro, Carmen Sanchez and Lucía Sánchez.

FUNDING

This work was supported by Instituto de Salud Carlos III (ISCIII), [grant numbers CP11/00080], Ministerio de Ciencia e Innovacion (MICINN) [grant numbers BFU2011-024760 and SAF2010-16377] and Fondo de Investigación Sanitaria (FIS)-Red Temática de Investigación Cooperativa en Enfermedades Cardiovasculares (RECAVA) [grant number RD12/0042/0019]. RECAVA and Ciberehd networks are funded by the Carlos III Health Institute.

REFERENCES

1 Haffner, S. M., Lehto, S., Ronnemaa, T., Pyorala, K. and Laakso, M. (1998) Mortality from coronary heart disease in subjects with type 2 diabetes and in nondiabetic subjects with and without prior myocardial infarction. N. Engl. J. Med. **339**, 229–234 CrossRef PubMed

2 Maya, L. and Villarreal, F. J. (2010) Diagnostic approaches for diabetic cardiomyopathy and myocardial fibrosis. J. Mol. Cell Cardiol. **48**, 524–529 CrossRef PubMed

3 Van Gaal, L. F., Mertens, I. L. and De Block, C. E. (2006) Mechanisms linking obesity with cardiovascular disease. Nature **444**, 875–880 CrossRef PubMed

4 Komers, R., Lindsley, J. N., Oyama, T. T., Schutzer, W. E., Reed, J. F., Mader, S. L. and Anderson, S. (2001) Immunohistochemical and functional correlations of renal cyclooxygenase-2 in experimental diabetes. J. Clin. Invest. **107**, 889–898 CrossRef PubMed

5 Vandanmagsar, B., Youm, Y. H., Ravussin, A., Galgani, J. E., Stadler, K., Mynatt, R. L., Ravussin, E., Stephens, J. M. and Dixit, V. D. (2011) The NLRP3 inflammasome instigates obesity-induced inflammation and insulin resistance. Nat. Med. **17**, 179–188 CrossRef PubMed

6 Pickup, J. C., Mattock, M. B., Chusney, G. D. and Burt, D. (1997) NIDDM as a disease of the innate immune system: association of acute-phase reactants and interleukin-6 with metabolic syndrome X. Diabetologia **40**, 1286–1292 CrossRef PubMed

7 Schertzer, J. D., Tamrakar, A. K., Magalhaes, J. G., Pereira, S., Bilan, P. J., Fullerton, M. D., Liu, Z., Steinberg, G. R., Giacca, A., Philpott, D. J. and Klip, A. (2011) NOD1 activators link innate immunity to insulin resistance. Diabetes **60**, 2206–2215 CrossRef PubMed

8 Wong, F. S., Hu, C., Zhang, L., Du, W., Alexopoulou, L., Flavell, R. A. and Wen, L. (2008) The role of Toll-like receptors 3 and 9 in the development of autoimmune diabetes in NOD mice. Ann. N.Y. Acad. Sci. **1150**, 146–148 CrossRef PubMed

Author Copy

9 Shi, H., Kokoeva, M. V., Inouye, K., Tzameli, I., Yin, H. and Flier, J. S. (2006) TLR4 links innate immunity and fatty acid-induced insulin resistance. J. Clin. Invest. **116**, 3015–3025 CrossRef PubMed

10 Dasu, M. R., Devaraj, S., Park, S. and Jialal, I. (2010) Increased Toll-like receptor (TLR) activation and TLR ligands in recently diagnosed type 2 diabetic subjects. Diabetes Care **33**, 861–868 CrossRef PubMed

11 Meylan, E., Tschopp, J. and Karin, M. (2006) Intracellular pattern recognition receptors in the host response. Nature **442**, 39–44 CrossRef PubMed

12 Correa, R. G., Khan, P. M., Askari, N., Zhai, D., Gerlic, M., Brown, B., Magnuson, G., Spreafico, R., Albani, S., Sergienko, E. et al. (2011) Discovery and characterization of 2-aminobenzimidazole derivatives as selective NOD1 inhibitors. Chem. Biol. **18**, 825–832 CrossRef PubMed

13 Harton, J. A., Linhoff, M. W., Zhang, J. and Ting, J. P. (2002) Cutting edge: CATERPILLER: a large family of mammalian genes containing CARD, pyrin, nucleotide-binding, and leucine-rich repeat domains. J. Immunol. **169**, 4088–4093 CrossRef PubMed

14 Carneiro, L. A., Magalhaes, J. G., Tattoli, I., Philpott, D. J. and Travassos, L. H. (2008) Nod-like proteins in inflammation and disease. J. Pathol. **214**, 136–148 CrossRef

15 Davis, B. K., Wen, H. and Ting, J. P. (2011) The inflammasome NLRs in immunity, inflammation, and associated diseases. Ann. Rev. Immunol. **29**, 707–735 CrossRef PubMed

16 Gatheral, T., Reed, D. M., Moreno, L., Gough, P. J., Votta, B. J., Sehon, C. A., Rickard, D. J., Bertin, J., Lim, E., Nicholson, A. G. and Mitchell, J. A. (2012) A key role for the endothelium in NOD1 mediated vascular inflammation: comparison to TLR4 responses. PLoS One **7**, e42386 CrossRef PubMed

17 Moreno, L., McMaster, S. K., Gatheral, T., Bailey, L. K., Harrington, L. S., Cartwright, N., Armstrong, P. C., Warner, T. D., Paul-Clark, M. and Mitchell, J. A. (2010) Nucleotide oligomerization domain 1 is a dominant pathway for NOS2 induction in vascular smooth muscle cells: comparison with Toll-like receptor 4 responses in macrophages. Br. J. Pharmacol. **160**, 1997–2007 CrossRef PubMed

18 Nishio, H., Kanno, S., Onoyama, S., Ikeda, K., Tanaka, T., Kusuhara, K., Fujimoto, Y., Fukase, K., Sueishi, K. and Hara, T. (2011) Nod1 ligands induce site-specific vascular inflammation. Arterioscler. Thromb. Vasc. Biol. **31**, 1093–1099 CrossRef PubMed

19 Moreno, L. and Gatheral, T. (2013) Therapeutic targeting of NOD1 receptors. Br. J. Pharmacol. **170**, 475–485 CrossRef PubMed

20 Ture-Ozdemir, F., Tulunay, A., Elbasi, M. O., Tatli, I., Maurer, A. M., Mumcu, G., Direskeneli, H. and Eksioglu-Demiralp, E. (2013) Pro-inflammatory cytokine and caspase-1 responses to pattern recognition receptor activation of neutrophils and dendritic cells in Behcet's disease. Rheumatology **52**, 800–805 CrossRef PubMed

21 Ver Heul, A. M., Fowler, A., Ramaswamy, S. and Piper, R. C. (2013) Ubiquitin regulates caspase recruitment domain mediated signaling by nucleotide binding oligomerization domain proteins NOD1 and NOD2. J. Biol. Chem. **288**, 6890–902 CrossRef PubMed

22 Fernandez-Velasco, M., Prieto, P., Terron, V., Benito, G., Flores, J. M., Delgado, C., Zaragoza, C., Lavin, B., Gomez-Parrizas, M., Lopez-Collazo, E. et al. (2012) NOD1 activation induces cardiac dysfunction and modulates cardiac fibrosis and cardiomyocyte apoptosis. PLoS One **7**, e45260 CrossRef PubMed

23 Inohara, N., Koseki, T., del Peso, L., Hu, Y., Yee, C., Chen, S., Carrio, R., Merino, J., Liu, D., Ni, J. and Nunez, G. (1999) Nod1, an Apaf-1-like activator of caspase-9 and nuclear factor-kappaB. J. Biol. Chem. **274**, 14560–14567 CrossRef PubMed

24 Zhao, L., Hu, P., Zhou, Y., Purohit, J. and Hwang, D. (2011) NOD1 activation induces proinflammatory gene expression and insulin resistance in 3T3-L1 adipocytes. Am. J. Physiol. Endocrinol. Metab. **301**, E587–E598 CrossRef PubMed

25 Shiny, A., Regin, B., Balachandar, V., Gokulakrishnan, K., Mohan, V., Babu, S. and Balasubramanyam, M. (2013) Convergence of innate immunity and insulin resistance as evidenced by increased nucleotide oligomerization domain (NOD) expression and signaling in monocytes from patients with type 2 diabetes. Cytokine **64**, 564–570 CrossRef PubMed

26 Fernandez-Velasco, M., Rueda, A., Rizzi, N., Benitah, J. P., Colombi, B., Napolitano, C., Priori, S. G., Richard, S. and Gomez, A. M. (2009) Increased Ca^{2+} sensitivity of the ryanodine receptor mutant RyR2R4496C underlies catecholaminergic polymorphic ventricular tachycardia. Circ. Res. **104**, 201–209 CrossRef PubMed

27 Zhou, Y. J., Zhou, H., Li, Y. and Song, Y. L. (2012) NOD1 activation induces innate immune responses and insulin resistance in human adipocytes. Diabetes Metab. **38**, 538–543 CrossRef PubMed

28 Cuda, C., Badawi, A., Karmali, M. and El-Sohemy, A. (2012) Effects of polymorphisms in nucleotide-binding oligomerization domains 1 and 2 on biomarkers of the metabolic syndrome and type II diabetes. Genes Nutr. **7**, 427–435 CrossRef PubMed

29 Amar, J., Chabo, C., Waget, A., Klopp, P., Vachoux, C., Bermudez-Humaran, L. G., Smirnova, N., Berge, M., Sulpice, T., Lahtinen, S. et al. (2011) Intestinal mucosal adherence and translocation of commensal bacteria at the early onset of type 2 diabetes: molecular mechanisms and probiotic treatment. EMBO Mol. Med. **3**, 559–572 CrossRef PubMed

30 Pereira, L., Matthes, J., Schuster, I., Valdivia, H. H., Herzig, S., Richard, S. and Gomez, A. M. (2006) Mechanisms of $[Ca^{2+}]i$ transient decrease in cardiomyopathy of db/db type 2 diabetic mice. Diabetes **55**, 608–615 CrossRef PubMed

31 Neubauer, N. and Kulkarni, R. N. (2006) Molecular approaches to study control of glucose homeostasis. ILAR J. **47**, 199–211 CrossRef PubMed

32 Leiter, E. H. and Reifsnyder, P. C. (2004) Differential levels of diabetogenic stress in two new mouse models of obesity and type 2 diabetes. Diabetes. **53** (Suppl. 1), S4–S11 CrossRef PubMed

33 Loskutoff, D. J., Fujisawa, K. and Samad, F. (2000) The fat mouse. A powerful genetic model to study hemostatic gene expression in obesity/NIDDM. Ann. N.Y. Acad. Sci. **902**, 272–281, discussion 281–272 CrossRef PubMed

34 Inohara, N., Ogura, Y., Chen, F. F., Muto, A. and Nunez, G. (2001) Human Nod1 confers responsiveness to bacterial lipopolysaccharides. J. Biol. Chem. **276**, 2551–2554 CrossRef PubMed

35 Jakopin, Z., Gobec, M., Kodela, J., Hazdovac, T., Mlinaric-Rascan, I. and Sollner Dolenc, M. (2013) Synthesis of conformationally constrained gamma-D-glutamyl-meso-diaminopimelic acid derivatives as ligands of nucleotide-binding oligomerization domain protein 1 (Nod1). Eur. J. Med. Chem. **69**, 232–243 CrossRef PubMed

36 Masumoto, J., Yang, K., Varambally, S., Hasegawa, M., Tomlins, S. A., Qiu, S., Fujimoto, Y., Kawasaki, A., Foster, S. J., Horie, Y. et al. (2006) Nod1 acts as an intracellular receptor to stimulate chemokine production and neutrophil recruitment *in vivo*. J. Exp. Med. **203**, 203–213 CrossRef PubMed

37 Pickup, J. C. and Crook, M. A. (1998) Is type II diabetes mellitus a disease of the innate immune system? Diabetologia **41**, 1241–1248 CrossRef PubMed

38 Xu, X. H., Shah, P. K., Faure, E., Equils, O., Thomas, L., Fishbein, M. C., Luthringer, D., Xu, X. P., Rajavashisth, T. B., Yano, J. et al. (2001) Toll-like receptor-4 is expressed by macrophages in murine and human lipid-rich atherosclerotic plaques and upregulated by oxidized LDL. Circulation **104**, 3103–3108 CrossRef PubMed

39 Edfeldt, K., Swedenborg, J., Hansson, G. K. and Yan, Z. Q. (2002) Expression of Toll-like receptors in human atherosclerotic lesions: a possible pathway for plaque activation. Circulation **105**, 1158–1161 PubMed

Author Copy

 © The Authors Journal compilation © 2014 Biochemical Society

40 Duewell, P., Kono, H., Rayner, K. J., Sirois, C. M., Vladimer, G., Bauernfeind, F. G., Abela, G. S., Franchi, L., Nunez, G., Schnurr, M. et al. (2010) NLRP3 inflammasomes are required for atherogenesis and activated by cholesterol crystals. Nature **464**, 1357–1361 CrossRef PubMed

41 Fritz, J. H., Ferrero, R. L., Philpott, D. J. and Girardin, S. E. (2006) Nod-like proteins in immunity, inflammation and disease. Nat. Immunol. **7**, 1250–1257 CrossRef PubMed

42 Kanneganti, T. D., Lamkanfi, M. and Nunez, G. (2007) Intracellular NOD-like receptors in host defense and disease. Immunity **27**, 549–559 CrossRef PubMed

43 Hysi, P., Kabesch, M., Moffatt, M. F., Schedel, M., Carr, D., Zhang, Y., Boardman, B., von Mutius, E., Weiland, S. K., Leupold, W. et al. (2005) NOD1 variation, immunoglobulin E and asthma. Hum. Mol. Genet. **14**, 935–941 CrossRef PubMed

44 Weidinger, S., Klopp, N., Rummler, L., Wagenpfeil, S., Novak, N., Baurecht, H. J., Groer, W., Darsow, U., Heinrich, J., Gauger, A. et al. (2005) Association of NOD1 polymorphisms with atopic eczema and related phenotypes. J. Allergy Clin. Immunol. **116**, 177–184 CrossRef PubMed

45 Girardin, S. E., Tournebize, R., Mavris, M., Page, A. L., Li, X., Stark, G. R., Bertin, J., DiStefano, P. S., Yaniv, M., Sansonetti, P. J. and Philpott, D. J. (2001) CARD4/Nod1 mediates NF-kappaB and JNK activation by invasive *Shigella flexneri*. EMBO Rep. **2**, 736–742 CrossRef PubMed

46 da Silva Correia, J., Miranda, Y., Austin-Brown, N., Hsu, J., Mathison, J., Xiang, R., Zhou, H., Li, Q., Han, J. and Ulevitch, R. J. (2006) Nod1-dependent control of tumor growth. Proc. Natl. Acad. Sci. U.S.A. **103**, 1840–1845 CrossRef PubMed

47 Cartwright, N., Murch, O., McMaster, S. K., Paul-Clark, M. J., van Heel, D. A., Ryffel, B., Quesniaux, V. F., Evans, T. W., Thiemermann, C. and Mitchell, J. A. (2007) Selective NOD1 agonists cause shock and organ injury/dysfunction *in vivo*. Am. J. Respir. Crit. Care Med. **175**, 595–603 CrossRef PubMed

48 Zhao, L., Kwon, M. J., Huang, S., Lee, J. Y., Fukase, K., Inohara, N. and Hwang, D. H. (2007) Differential modulation of Nods signaling pathways by fatty acids in human colonic epithelial HCT116 cells. J. Biol. Chem. **282**, 11618–11628 CrossRef PubMed

49 Hasegawa, M., Fujimoto, Y., Lucas, P. C., Nakano, H., Fukase, K., Nunez, G. and Inohara, N. (2008) A critical role of RICK/RIP2 polyubiquitination in Nod-induced NF-kappaB activation. EMBO J. **27**, 373–383 CrossRef PubMed

50 Magalhaes, J. G., Lee, J., Geddes, K., Rubino, S., Philpott, D. J. and Girardin, S. E. (2011) Essential role of Rip2 in the modulation of innate and adaptive immunity triggered by Nod1 and Nod2 ligands. Eur. J. Immunol. **41**, 1445–1455 CrossRef PubMed

51 Park, J. H., Kim, Y. G., Shaw, M., Kanneganti, T. D., Fujimoto, Y., Fukase, K., Inohara, N. and Nunez, G. (2007) Nod1/RICK and TLR signaling regulate chemokine and antimicrobial innate immune responses in mesothelial cells. J. Immunol. **179**, 514–521 CrossRef PubMed

52 Nembrini, C., Kisielow, J., Shamshiev, A. T., Tortola, L., Coyle, A. J., Kopf, M. and Marsland, B. J. (2009) The kinase activity of Rip2 determines its stability and consequently Nod1- and Nod2-mediated immune responses. J. Biol. Chem. **284**, 19183–19188 CrossRef PubMed

53 Barouch, L. A., Gao, D., Chen, L., Miller, K. L., Xu, W., Phan, A. C., Kittleson, M. M., Minhas, K. M., Berkowitz, D. E., Wei, C. and Hare, J. M. (2006) Cardiac myocyte apoptosis is associated with increased DNA damage and decreased survival in murine models of obesity. Circ. Res. **98**, 119–124 CrossRef PubMed

54 da Silva Correia, J., Miranda, Y., Leonard, N., Hsu, J. and Ulevitch, R. J. (2007) Regulation of Nod1-mediated signaling pathways. Cell Death Differ. **14**, 830–839 CrossRef PubMed

55 Frantz, S., Kobzik, L., Kim, Y. D., Fukazawa, R., Medzhitov, R., Lee, R. T. and Kelly, R. A. (1999) Toll4 (TLR4) expression in cardiac myocytes in normal and failing myocardium. J. Clin. Invest. **104**, 271–280 CrossRef PubMed

56 Larsen, C. M., Faulenbach, M., Vaag, A., Volund, A., Ehses, J. A., Seifert, B., Mandrup-Poulsen, T. and Donath, M. Y. (2007) Interleukin-1-receptor antagonist in type 2 diabetes mellitus. N. Engl. J. Med. **356**, 1517–1526 CrossRef PubMed

Received 27 March 2014/21 May 2014; accepted 17 June 2014

Published as Immediate Publication 17 June 2014, doi: 10.1042/CS20140180

Author Copy

Clinical Science (2014) **127**, 665–677 (Printed in Great Britain) doi: 10.1042/CS20140180

online data

Original Paper

SUPPLEMENTARY ONLINE DATA

NOD1 receptor is up-regulated in diabetic human and murine myocardium

Patricia PRIETO*, María Teresa VALLEJO-CREMADES†[1], Gemma BENITO†[1], Pilar GONZÁLEZ-PERAMATO‡, Daniel FRANCÉS*, Noelia AGRA*, Verónica TERRÓN*, Silvia GÓNZALEZ-RAMOS*, Carmen DELGADO§, Mariano RUIZ-GAYO¶, Ivette PACHECO**, Juan P. VELASCO-MARTÍN††, Javier REGADERA††, Paloma MARTÍN-SANZ*, Eduardo LÓPEZ-COLLAZO†, Lisardo BOSCÁ* and María FERNÁNDEZ-VELASCO†

*Instituto de Investigaciones Biomédicas Alberto Sols, Centro Mixto CSIC-UAM, Madrid, Spain
†Instituto de Investigación Hospital Universitario La Paz (IDIPAZ), Madrid, Spain
‡Departamento de Anatomía Patológica, Hospital Universitario La Paz, Universidad Autonoma de Madrid, Madrid, Spain
§Centro de Investigaciones Biológicas. Facultad de Medicina, Universidad Complutense de Madrid, Madrid, Spain
¶Universidad CEU San Pablo, Madrid, Spain
**Hospital Militar de Managua, Managua, Nicaragua
††Departamento de Anatomía, Histología y Neurociencia, Facultad de Medicina, Universidad Autónoma de Madrid, Madrid Spain

Author Copy

MATERIALS AND METHODS

HFD feeding

For the high-fat diet (HFD) exeriments, 4-week-old C57BL/6J male mice (wt) weighing 16–18 g were housed under a 12/12-h light–dark cycle in a temperature-controlled room (22 °C), with standard food and water available *ad libitum*. Mice were divided into two groups of similar average body weight, housed four per cage and assigned to either a control regular chow diet or a 42% HFD (TD. 88137, Harlan Laboratories). Body weight and food intake were monitored once per week. After 12 weeks of treatment, mice were killed, and heart tissues were snap-frozen in liquid nitrogen and stored at − 80 °C.

Glucose and insulin determination

Plasma glucose was measured in a Reflotron plus (Roche). Insulin was quantified with the Rat/Mouse Insulin 96-Well Plate Assay Kit.

Immunofluorescence staining

HL-1 cells were seeded on to sterile eight-well Chamber Slides (Falcon) and fixed with 2% paraformaldehyde for 10 min. Cells were permeabilized in ice-cold methanol and incubated with 3% BSA for 30 min. After incubation with a rabbit antibody against glucose transporter 4 (GLUT-4) (1:500 dilution; Abcam) at 4 °C overnight, cells were washed with PBS followed by incubation with Alexa Fluor® 488-conjugated goat anti-rabbit secondary antibody (1:500 dilution; Molecular Probes) for 1 h at room temperature. Coverslips were mounted in Prolong Gold antifade reagent (Molecular Probes) and examined using a Leica TCS SP5 spectral confocal microscope. Alexa Fluor® fluorescence was excited using the 488 nm line of an argon laser and emission collected through a band-pass filter (505–530 nm). DAPI fluorescence was excited using a mercury lamp (band-pass 365/12) and emissions collected through a band-pass filter (480–520 nm). Fluorescence intensity measurements were performed using ImageJ software (NIH).

Immunohistochemistry of human samples

Samples were deparaffinized and then blocked by incubation for 60 min at room temperature with TBS, at pH 7.6, containing 10% goat serum and 1.5% BSA. Sections were then incubated overnight at 4 °C with an anti-NOD1 antibody followed by three 5-min washes with TBS. Bound primary antibody was detected by incubation for 45 min with biotinylated horse anti-goat secondary antibody (1:50 dilution; Vector Laboratories), followed by three 5-min washes with TBS and then incubation for 30 min with streptavidin conjugated to Alexa Fluor® 488 (1:1000 dilution; Molecular Probes). Slides were washed again three times in TBS, rinsed once briefly in water and mounted under a coverslip with VectaShield mounting medium with DAPI (Vector Laboratories). Samples were visualized by epifluorescence microscopy. Epifluorescence microscopy was performed on a Leica AF6000 by using a ×20 dry objective lens. Emission/excitation filters for DAPI and Alexa Fluor® 488 were used. A sample with no primary antibody was always included to control for background generated by the secondary antibody.

Quantification of lipid incorporation by HL-1 cells

Accumulation of lipid by HL-1 cells was determined using the lipophilic Nile Red fluorescent dye. Cells were incubated for 48 h with 50 mmol/l glucose and 200 μmol/l palmitic acid. HL-1 cells were trypsinized and centrifuged for 5 min at 200 ***g*** at 4 °C. Cell pellets were re-suspended and fixed with 2% paraformaldehyde at 4 °C. For flow cytometry, cells were sedimented as described above, re-suspended in PBS with a final Nile Red concentration of 0.4 μg/ml (30 min). Fluorescence emission was

[1]**These authors contributed equally to the study.**

Correspondence: Dr María Fernández-Velasco (email mvelasco@iib.uam.es or maria.fernandez@idipaz.es) or Professor Lisardo Boscá (email lbosca@iib.uam.es).

© The Authors Journal compilation © 2014 Biochemical Society

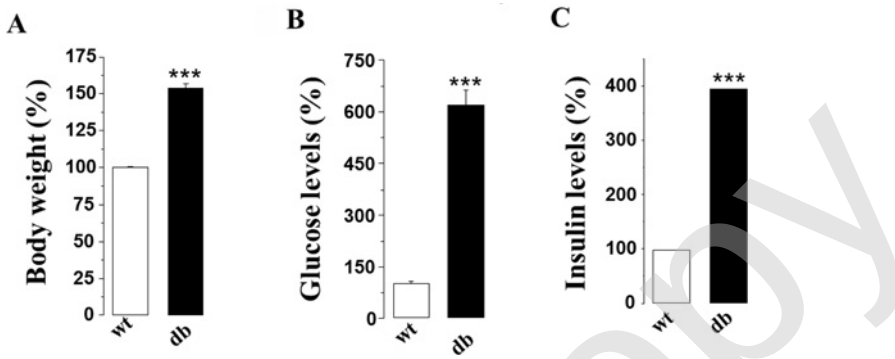

Figure S1 **Body weight and plasma levels of glucose and insulin in *db* mice**
Body weight (**A**), glucose (**B**) and insulin (**C**) plasma levels obtained in *db* mice. Data are expressed as means ± S.E.M. of the percentage of the corresponding wt mice (100%). ***$P < 0.001$ compared with their corresponding wt mice.

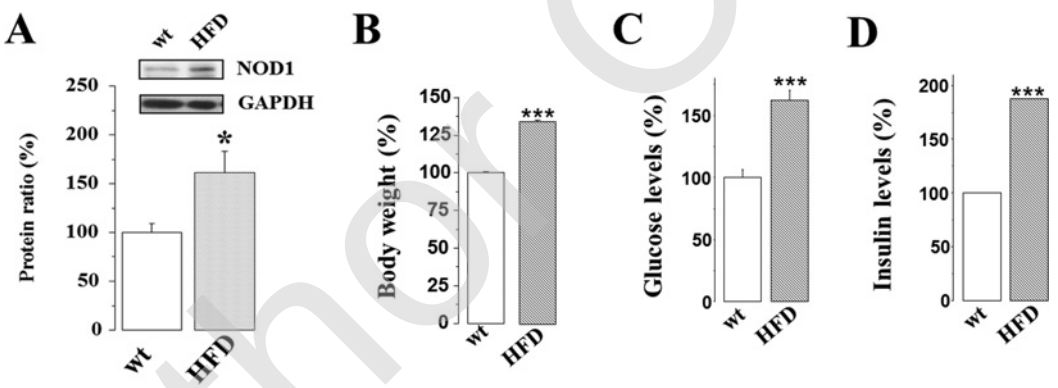

Figure S2 **NOD1 protein expression, body weight, and plasma levels of glucose and insulin obtained in HFD-treated mice**
Representative immunoblot and average data of NOD1/GAPDH expression obtained in cardiac tissue of wt mice and HFD-fed mice (**A**). Body weight (**B**), and glucose (**C**) and insulin (**D**) plasma levels obtained in HFD-fed mice for 12 weeks. Data are expressed as means ± S.E.M. of the percentage of the corresponding wt mice (100%). *$P < 0.05$ and ***$P < 0.001$ compared with the corresponding *wt*.

detected between 564 nm and 604 nm with band-pass filter using FACScan flow cytometer (FC-500 Becton Dickinson). Data analysis was presented using forward scatter (FSC) compared with fluorescence, where the percentage of lipid accumulation was calculated on the basis of the cells stained with high fluorescence values.

Author copy

© The Authors Journal compilation © 2014 Biochemical Society

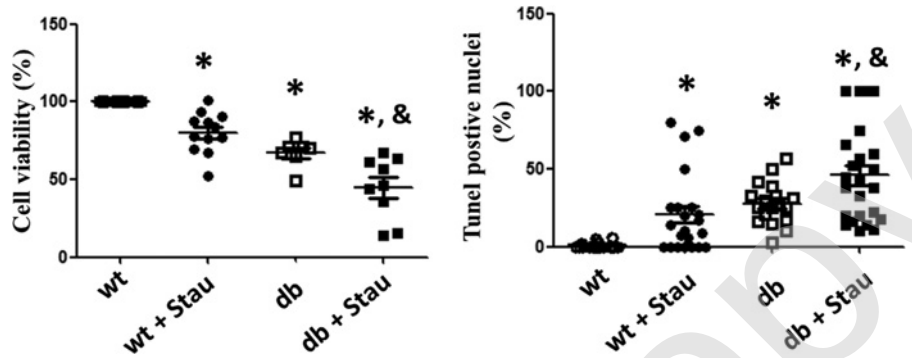

Figure S3 Staurosporine induces apoptosis in isolated native cardiomyocytes
Staurosporine (100 ng/ml) decreases cell viability (left panel) and increases the TUNEL-positive nuclei (right panel) in cardiomyocytes from wt and *db* mice. Data are expressed as means ± S.E.M. of the percentage of the corresponding wt mice (100 %); $n = 3$–5 animals per condition. $^{*}P < 0.05$ compared with wt mice; $^{\&}P < 0.05$ compared with *db* mice.

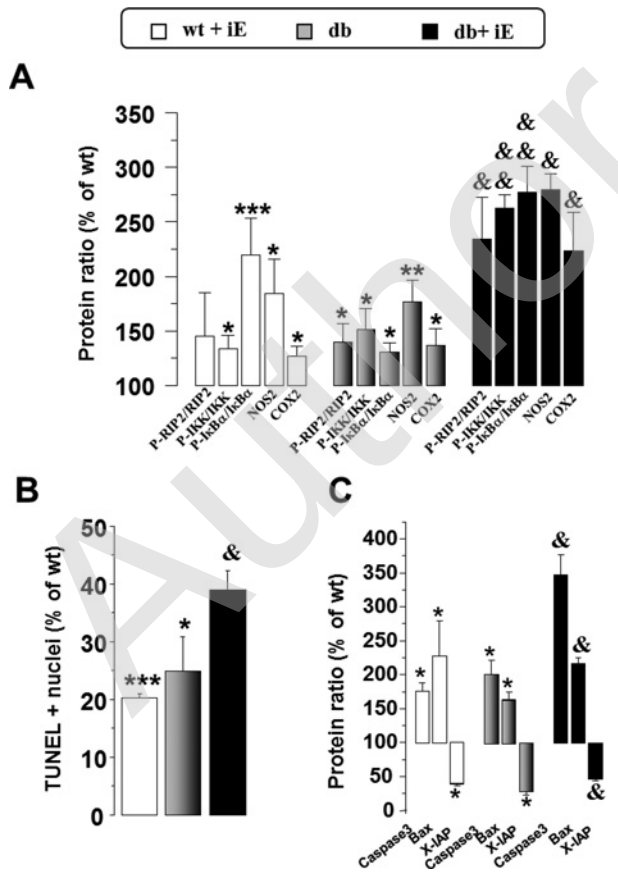

Figure S4 Selective stimulation of NOD1 induces NF-κB and apoptotic pathway activation
Animals received intraperitoneal iEDAP (5 μg/g of body weight; iE), a selective agonist of NOD1, or vehicle. After 2 weeks of treatment up-regulation of phospho-RIP2/RIP2, phospho-IKK/IKK, phospho-IκBα/IκBα, NOS2 and COX2 proteins were observed in hearts from wt and *db* mice (**A**). IE administration also promoted an increase in the number of TUNEL-positive nuclei (**B**), caspase-3 and BAX levels, and a decrease in X-IAP protein levels (**C**). Data are expressed as means ± S.E.M. compared with the corresponding wt mice (100 %). $^{*}P < 0.05$ compared with wt mice; $^{\&}P < 0.05$ compared with *db* mice; $n = 4$–6 animals.

Author copy

© The Authors Journal compilation © 2014 Biochemical Society

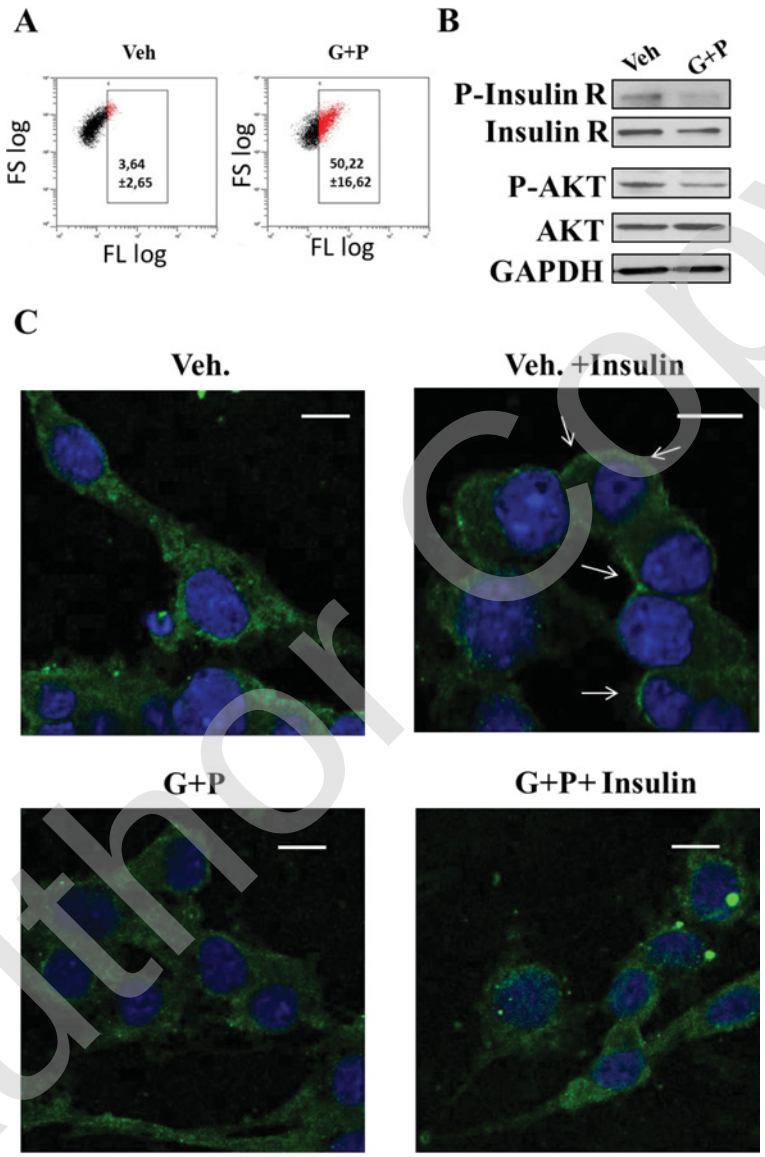

Figure S5 **HL-1 cells incubated with palmitate and glucose reveal changes in insulin signalling and lipid accumulation**
(**A**) Nile Red fluorescence staining demonstrates lipid incorporation in HL-1 cells incubated for 48 h with 50 mmol/l glucose and 200 μmol/l palmitate. Left panel shows an example obtained in vehicle-treated cells (Veh.) and the right panel illustrates an example obtained in cells incubated with glucose and palmitate (G + P). The mean values have been added to the Figure ($n = 3$). (**B**) Representative immunoblots of phospho-Akt/Akt, phospho-InsulinR/InsulinR (insulin receptor) and GAPDH from cells treated for 48 h with Veh. or with 50 mmol/l glucose and 200 μmol/l palmitate (G + P) and treated with insulin (100 nmol/l) for 5 min prior to collection. Insulin failed to phosphorylate both the Akt and InsulinR in G + P-treated cells. Representative immunoblots from three different experiments. (**C**) Immunofluorescence of GLUT-4 in HL-1 cells incubated with 50 mmol/l glucose and 200 μmol/l palmitate (G + P) for 48 h and treated with insulin (100 nmol/l) for 5 min. Vehicle-treated cells (Veh.) incubated with insulin for 5 min showed a prominent GLUT-4 transmembrane localization (arrows) compared with vehicle-treated cells under basal conditions (left panel). G + P-treated cells incubated with insulin did not show GLUT-4 transmembrane localization, suggesting that G + P-treatment induces an impairment in insulin-induced glucose transporter localization.

Author Copy

© The Authors Journal compilation © 2014 Biochemical Society

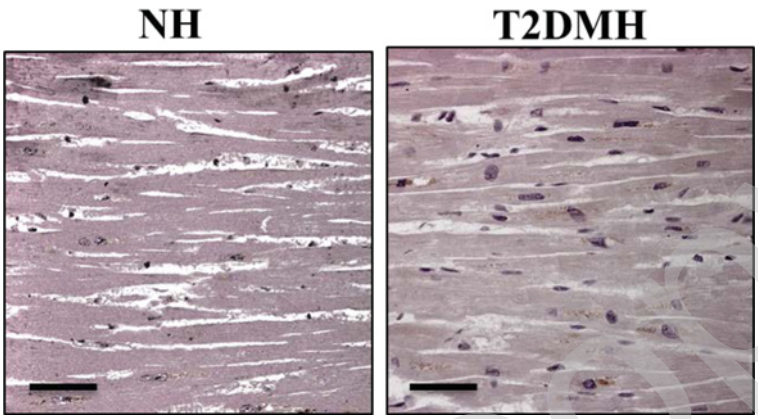

Figure S6 **Negative control for NOD1 immunohistochemistry staining**
Longitudinal heart section incubated with a mouse IgG instead of the primary antibody for NOD1. Scale = 100 μm.

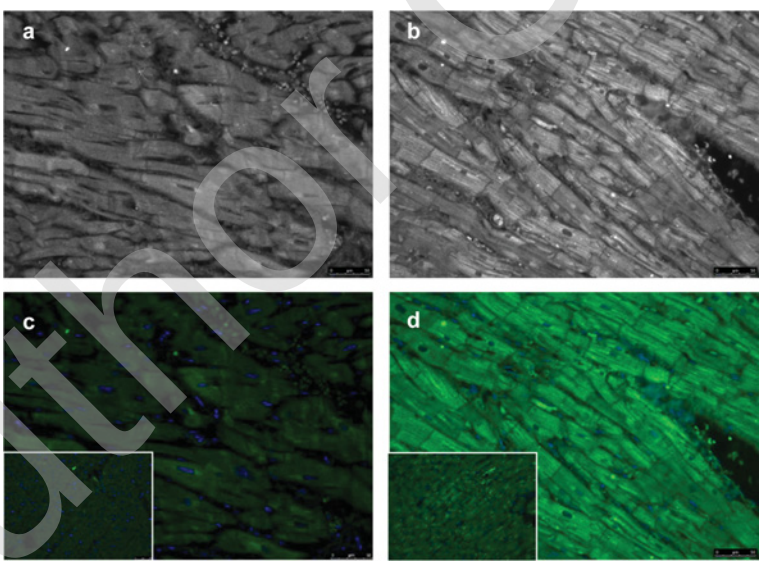

Figure S7 **NOD1 is up-regulated in the myocardium of T2DMH**
Myocardial sections of NH and T2DMH were stained with a NOD1 antibody (×40). Bright-field phase-contrast images are shown in panels (**a**) and (**b**). NOD1 staining revealed high expression of this NLR in T2DMH compared with NH (**c**, **d**). Negative controls obtained for each sample are shown in the insets.

Received 27 March 2014/21 May 2014; accepted 17 June 2014
Published as Immediate Publication 17 June 2014, doi: 10.1042/CS20140180

Author copy

© The Authors Journal compilation © 2014 Biochemical Society